



Spin Properties and Metal-Semiconductor Transition of Nitrogen-Containing Zigzag Graphyne Nanoribbon Caused by Magnetic Atom Doping

Zi-Cong Min, Xiao-Fang Peng* and Shi-Hua Tan*

Hunan Provincial Key Laboratory of Materials Surface or Interface Science and Technology, College of Materials Science and Engineering, Central South University of Forestry and Technology, Changsha, China

OPEN ACCESS

Edited by:

Ke-Qiu Chen,
Hunan University, China

Reviewed by:

Zhou Guanghui,
Hunan Normal University, China
Z.H Zhang,
Changsha University of Science and
Technology, China

*Correspondence:

Xiao-Fang Peng
xiaofangpeng@163.com
Shi-Hua Tan
shtan@csuft.edu.cn

Specialty section:

This article was submitted to
Quantum Materials,
a section of the journal
Frontiers in Materials

Received: 14 January 2022

Accepted: 02 February 2022

Published: 30 March 2022

Citation:

Min Z-C, Peng X-F and Tan S-H (2022)
Spin Properties and Metal-
Semiconductor Transition of Nitrogen-
Containing Zigzag Graphyne
Nanoribbon Caused by Magnetic
Atom Doping.
Front. Mater. 9:854656.
doi: 10.3389/fmats.2022.854656

In this study, the density function theory (DFT) was used to study the influence of the magnetic atoms (Fe, Co, Ni) doping on the electrical properties of nitrogen-containing zigzag graphyne-like nanoribbon (N-ZGyNR). The results show that, by doping different atoms into the natural “holes” of N-ZGyNR, the changes in the structure, magnetic moment distribution and electrical properties of N-ZGyNR are different. Due to the incomplete saturation of the edge C atoms, the initial N-ZGyNR presents metallicity and spin degeneracy. The doping of Fe atoms will cause the C-C bond in N-ZGyNR to be completely broken, resulting in structural distortion, and about 0.8e⁻ will transfer from Fe to N-ZGyNR. Compared with Fe doping, Co/Ni doping has a smaller effect on the N-ZGyNR and will not cause structural distortion, but will redistribute the spin charge in N-ZGyNR, thereby forming a band gap of 60 meV near the Fermi level to realize the transition of metal-semiconductor. The above results show that the electrical properties of N-ZGyNR can be controlled by magnetic atom doping, and the metal-semiconductor transition can be realized by Co/Ni doping, which provides a new alternative for spintronic devices.

Keywords: nitrogen-containing graphyne, magnetic atom doping, metal-semiconductor transition, spin characterization, first-principles calculation

INTRODUCTION

In recent years, the research on graphene and graphyne has become the focus of attention in the new carbon isomorphous nanostructures. Graphyne is a new kind of carbon nanostructure material, which contains a large number of carbon chemical bonds. Its structure has the characteristics of large conjugated system, wide surface spacing, and stable chemical properties and semiconductor properties. In the 1980s, Baughman et al. (1987) proposed the concept of graphyne for the first time, predicting that graphyne has high temperature dynamic stability and high synthesis probability. Unlike graphene with sp²-hybridized carbon atoms, there are sp- and sp²-hybridized carbon atoms in graphynes, which make it completely different from graphene in geometry and physical properties (Li et al., 2014a; Bhattacharya et al., 2015). For example, four known graphyne lattice structures have been widely reported, namely, α , β , γ and 6,6,12-Graphyne (Baughman et al., 1987; Narita et al., 1998; Malko et al., 2012; Wu et al., 2013; Puigdollers et al., 2016).

Like graphene nanoribbons (GNRs), graphynes nanoribbons (GyNRs) are also realized by cutting graphyne sheets along the zigzag or armchair edges. GyNRs can have unusual magnetic, electronic properties such as magnetic/nonmagnetic or edge-dependent metal/semiconductor behavior (Zhang and Ma, 2011; Yue et al., 2012; Sarma et al., 2014; Sevinçli and Sevik, 2014; Wang et al., 2015; Li et al., 2020). Wu et al. (2013) studied the magnetic, electronic and transport properties of all types of GyNRs devices. They found that there was negative differential resistance effect (NDR) appeared in all other types of GyNRs except for α - and 6,6,12-GyNRs. Xi et al. (2014) used Wannier interpolation technique to study the electron-phonon coupling and charge transport properties of α and γ graphyne nanoribbons, and speculated that the electron mobility of α and γ graphynes reached $\sim 10^4 \text{ cm}^2 \text{ V}^{-1} \text{ s}^{-1}$ at room temperature. Through the above studies, it is shown that the graphyne system may have more amazing electrical properties than graphene, so graphyne is often regarded as a material for the production of carbon-based electronic devices.

One-dimensional/two-dimensional doped carbon materials have attracted more and more attention due to their structural diversity and unique electronic properties (Nayebi and Shamshirsaz, 2020; Chang et al., 2021). Haji-Nasiri and Fotoohi (Haji-Nasiri and Fotoohi, 2018) studied the transport properties of α -Armchair GyNRs (α -AGyNRs) devices doped with B and N atoms. They found that rectifying properties strongly depend on the location of defects (doped atoms). Qi et al. (2019) proposed a new two-dimensional carbonitride structure. The structure is composed of sp and sp²-hybrid carbon atoms and nitrogen atoms, with kagome, rhombus and hexagonal lattice. The first-principles calculations of these structures show that these two-dimensional nitrogen-containing graphynes are direct band gap semiconductors. At the same time, it is also found that in the two-dimensional diamond-shaped graphyne structure, the carrier mobility is the same as that of graphene, and the tensile strength is higher than that of graphene.

The study of magnetic properties of materials plays an important role in spintronics, which can contribute to the study of electronic transport in spin filters. In graphene or graphynes nanoribbons, the magnetic changes of nanoribbons can be realized by applying the applied transverse electric field (Son et al., 2006; Yue et al., 2012), boundary modification (Kan et al., 2008; Dutta et al., 2009; Deng et al., 2014; Krause et al., 2021), interface effect (Li et al., 2015; Wang et al., 2016; Zakharov, 2021) or adding various defects (Wang et al., 2009; Lin and Ni, 2011; Li and Zhang, 2013; Li et al., 2014b; Zhao et al., 2017; Jing et al., 2020; Liu et al., 2021). These methods effectively offset the local state energy of carbon atoms at the boundary to realize the magnetic transformation, and the most commonly used and efficient methods are doping and adsorption (Cocchi et al., 2010; Li and Zhang, 2013; Donati et al., 2014; Lin et al., 2014; Lazić and Crljen, 2015; Pan et al., 2015; Zhao et al., 2017; Jing et al., 2020; Liu et al., 2021). The doping method is used to study the electromagnetic changes of graphene and graphyne systems.

In this paper, inspired by the above research work, the effects of magnetic atoms (Fe, Co and Ni) doped in the structure of one-dimensional nitrogen-containing zigzag graphene-like nanoribbon (N-ZGyNR) on their electrical and magnetic properties are studied. The emphasis is on the magnetic interaction between the doped atoms and the boundary state, which will bring possibilities for the study of electronic devices of graphyne-like nanoribbon (GyNR).

SIMULATION MODEL AND CALCULATION METHOD

There are many large natural “holes” in the N-ZGyNR, which can be doped with magnetic atoms to adjust the electromagnetic properties. The geometric structure of M-N-ZGyNR is given in **Figures 1A–D**,

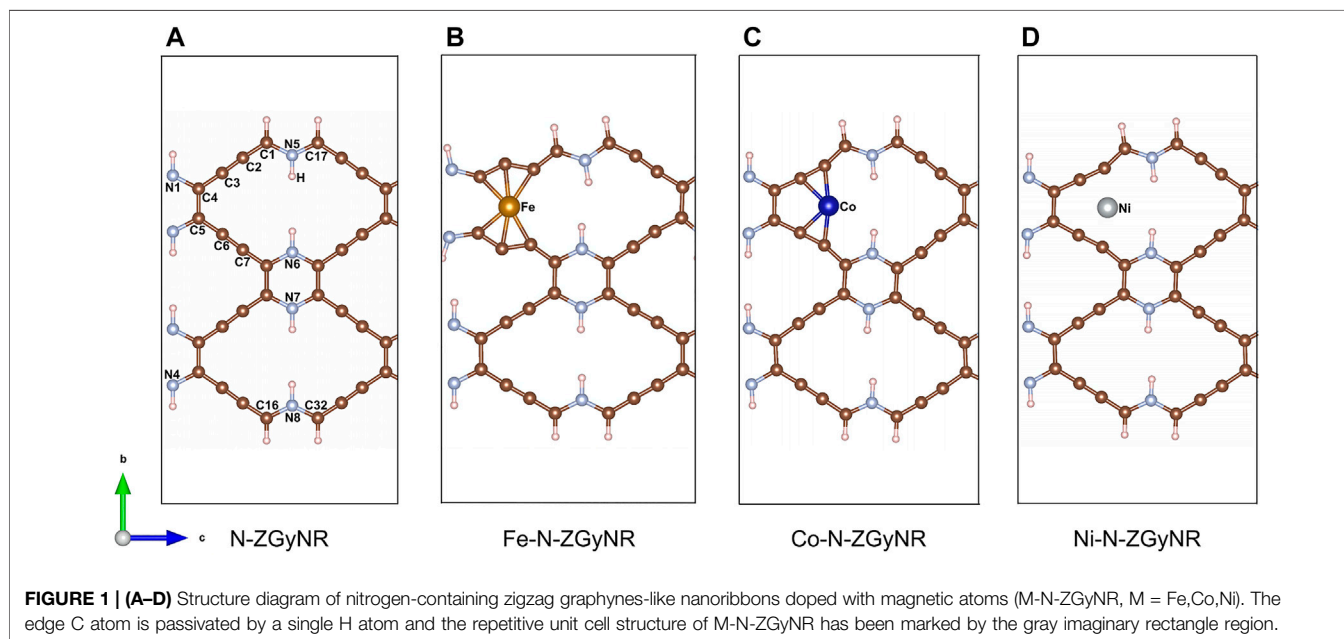


TABLE 1 | The formation energies of M-N-ZGyNR.

Configuration	ΔE (meV/atom)
Fe-N-ZGyNR	-52.45
Co-N-ZGyNR	-54.34
Ni-N-ZGyNR	-58.11

where the M atoms represent the doped magnetic atoms ($M = \text{Fe}, \text{Co}, \text{Ni}$). We know that for graphene or graphyne compound nanoribbons, the electron occupation at the edge of the carbon atom controls the spin polarized transmission. In our study, the initial spin of the N-ZGyNR is in the antiferromagnetic state, that is, the upper two C atoms (C_1 and C_{17}) are set to spin-up, and the lower two C atoms (C_{16} and C_{32}) are set to spin-down. In order to study the effect of embedded magnetic atoms on the boundary states near the Fermi level, we choose the natural “hole” near the edge carbon atom as the doping object. Due to symmetry (**Supplementary Figure S1**), the case that the initial spin of the magnetic atom is set to spin-up is only discussed. The repetitive unit cell structure has been enclosed by a rectangular dotted line. Each edge C atoms is passivated by a single hydrogen atom, and a large enough vacuum region in the x and y directions is given to prevent any interaction between the studied structure and its mirror image. The formation energies of the structures ($\Delta E_{M-N-ZGyNR}$) involved in this study are as follows:

$$\Delta E_{M-N-ZGyNR} = E_{M-N-ZGyNR} - E_{N-ZGyNR} - E_M \quad (1)$$

$E_{M-N-ZGyNR}$, $E_{N-ZGyNR}$ and E_M represent the total energy of N-ZGyNR doped with magnetic atoms M, pure N-ZGyNR structure without magnetic atoms and the isolated atoms M, respectively. In **Table 1**, we show the formation energies of M-N-ZGyNR $\Delta E_{M-N-ZGyNR}$. It can be found from **Table 1** that all the formation energies of M-N-ZGyNR are negative and much larger

than room temperature disturbances (~ 25 meV/atom), which means that the M-N-ZGyNR are stable at room temperature.

The spin electron density (SED) of M-N-ZGyNR, which can determine the type and size of the spin charge on each atom, can be calculated from the spin-up/spin-down charge density $\rho_{\uparrow/\downarrow}$

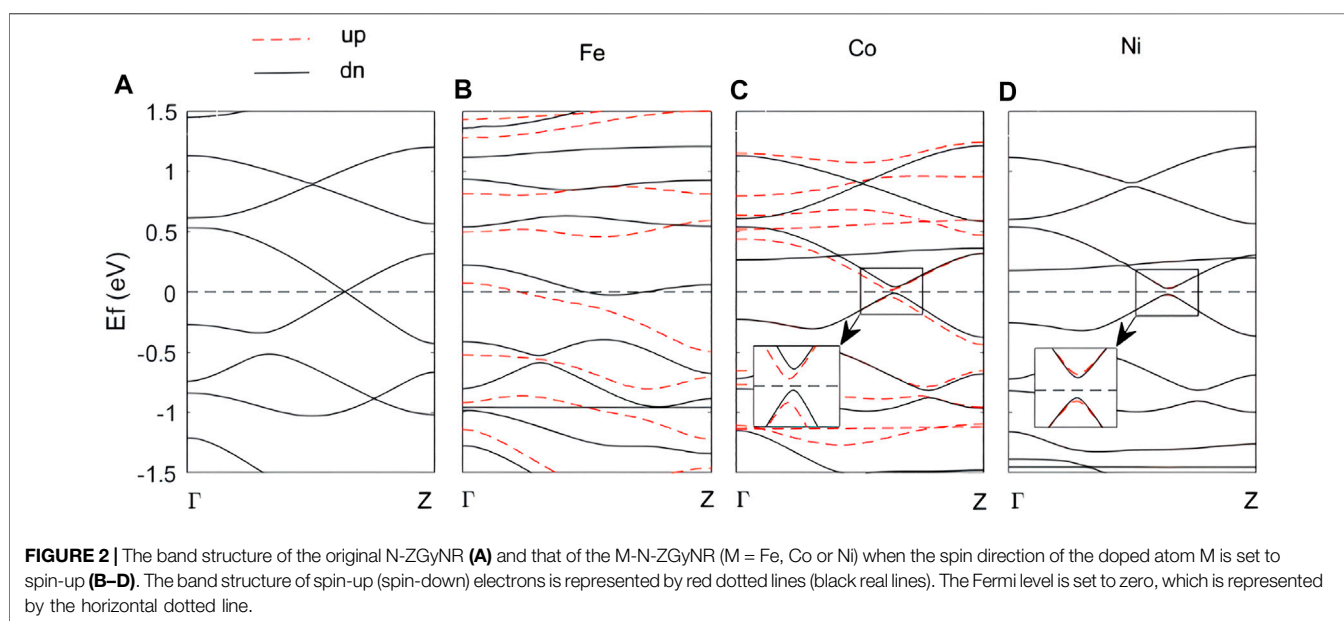
$$\Delta \rho^{\text{SED}} = \rho_{\uparrow} - \rho_{\downarrow} \quad (2)$$

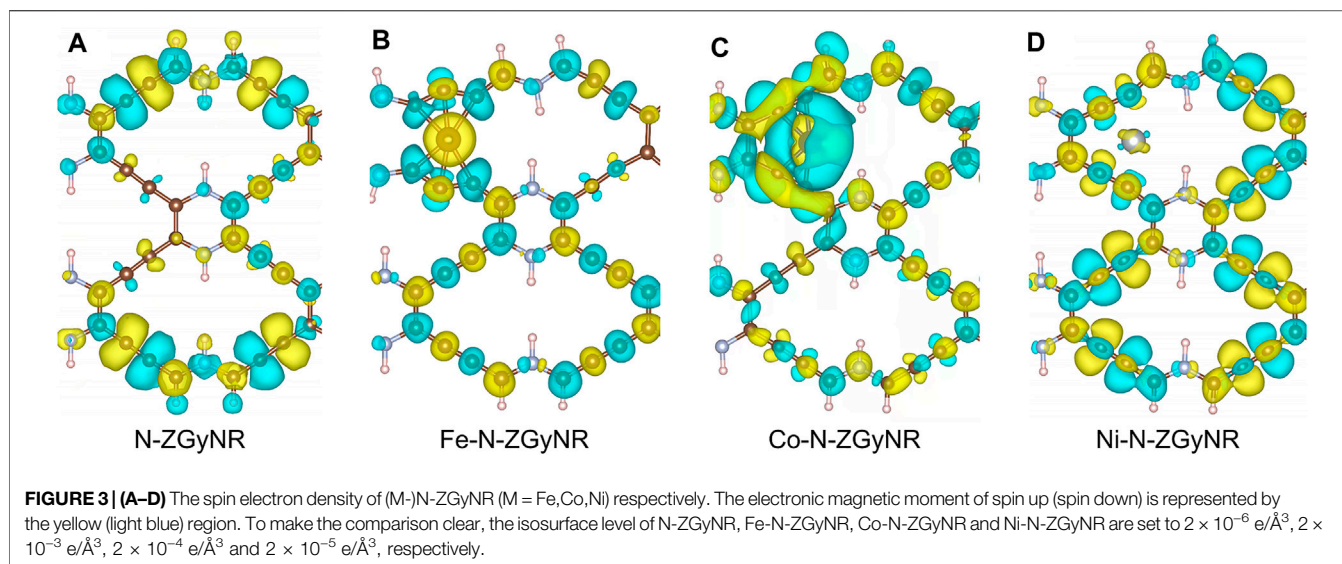
and the spin electron density difference (SEDD) of M-N-ZGyNR, which can get the total charge transfer before and after magnetic atom doping, is defined as

$$\Delta \rho_{M-N-ZGyNR}^{\text{SEDD}} = \rho_{M-N-ZGyNR} - \rho_{N-ZGyNR} - \rho_M \quad (3)$$

Here the $\rho_{M-N-ZGyNR}$, $\rho_{N-ZGyNR}$ and ρ_M represent the total electron density of M-N-ZGyNR, N-ZGyNR and the doped atom M, respectively.

In this work, all the first-principles calculations are performed by the Vienna Ab Initio Simulation Package (VASP) (Kresse and Furthmüller, 1996; Ren et al., 2019) with PAW potentials (Kresse and Joubert, 1999) and Strongly Constrained and Appropriately Normed Semilocal Density Functional (SCAN) (Young and Kane, 2015). The cutoff energy is set to 500eV in all calculations. The convergence criterion of force adopts quasi-Newton method for structural relaxation until the force tolerance reaches 0.02 eV/Å. The K grid sampling used in optimization and static calculations is $1 \times 1 \times 11$. In the energy band calculation, 30 K-points were taken along the z direction, and in the Co/Ni doping, an additional 20 K-points were taken near the band gap to confirm the existence of the band gap. The spin electron density distribution and spin electron distribution difference diagram are processed by VESTA (Momma and Izumi, 2011).





RESULTS AND DISCUSSION

Band Structure Analysis

The band structures of M-N-ZGyNR (M = Fe, Co and Ni) are shown in **Figure 2** (the red dotted lines represent the spin-up bands, and the black solid lines represent the spin-down bands). The band structure of the N-ZGyNR is given in **Figure 2A** for comparison. The lengths of $C_1(\text{sp})-C_2(\text{sp})$, $C_2(\text{sp})\equiv C_3(\text{sp})$, $C_3(\text{sp})-C_4(\text{sp})$, $C_4(\text{sp}^2) = C_5(\text{sp}^2)$ bonds in N-ZGyNR (The atomic label is shown in **Figure 1A**) are 1.35, 1.24, 1.36, 1.42 Å, respectively, which is in good agreement with those reported in the previous literature (Sevinçli and Sevik, 2014). All the atoms in N-ZGyNR are saturated and bonded, except for the C atoms on the edge. Take the C_1 as an example, it only has $C_1(\text{sp})-C_2(\text{sp})$, $C_1-\text{H}$, $C_1-\text{N}$ bonds. Combined with the inversion symmetry of the entire structure, N-ZGyNR exhibits spin-degenerate metallicity (in **Figure 2A**).

During the Fe doping process, the interaction between Fe and C atoms will cause significant structural distortions in N-ZGyNR (in **Figure 1B**). For example, the C_3 and C_6 will be pushed away (The atomic label is the same as N-ZGyNR in **Figure 1A**). The distance between C_4 and C_5 will increase from 1.42 Å to 2.59 Å, indicating that the $C_4(\text{sp}^2) = C_5(\text{sp}^2)$ bond is completely broken. The bond lengths of $C_2(\text{sp})\equiv C_3(\text{sp})$ and $C_6(\text{sp})\equiv C_7(\text{sp})$ will increase from ~ 1.24 Å to ~ 1.34 Å and becomes a C(sp)-C(sp) bond. With the larger structural relaxation changes in Fe-N-ZGyNR, the electronic band structure will also change significantly (in **Figure 2B**). When the doping atoms change from Fe to Co and Ni, the structural distortion is only limited to C_2-C_3 and C_6-C_7 , which are very close to the dopant atoms. Similar to Fe-N-ZGyNR, the bond lengths of C_2-C_3 and C_6-C_7 in Co/Ni-N-ZGyNR changed from triple bonds (1.24 Å) to single bonds (1.30 Å). With the destruction of the triple bond, an electronic band gap of 60 meV appears in Co-N-ZGyNR and Ni-N-ZGyNR (in **Figures 2C,D**), indicating that the electrical properties of the original N-ZGyNR changed from metal to semiconductor. The existence of the band gap value in Co/Ni-N-ZGyNR also can be confirmed from the dense density of states

curves (**Supplementary Figure S2**). These results indicate that the electrical properties of N-ZGyNR can be effectively controlled and designed for the metal-semiconductor transition through magnetic atom doping.

Spin Electron Density Analysis

To study the influence of doped magnetic atoms on the spin properties of N-ZGyNR, we calculated the spin electron density distribution of M-N-ZGyNR. The spin electron density distribution $\Delta\rho^{\text{SED}}$ by **Eq. 2** is used to intuitively describe the distribution of magnetic moment in the structure, as shown in **Figure 3**. The spin electron density distribution of the original N-ZGyNR structure is given in **Figure 3A** as a comparison. Here the yellow (light blue) part represents the spin-up (spin-down) magnetic moment, respectively. It should be noted that the isosurface levels from large to small are Fe-N-ZGyNR ($2 \times 10^{-3} e/\text{\AA}^3$), Co-N-ZGyNR ($2 \times 10^{-4} e/\text{\AA}^3$), Ni-N-ZGyNR ($2 \times 10^{-5} e/\text{\AA}^3$) and N-ZGyNR ($2 \times 10^{-6} e/\text{\AA}^3$) to make the comparison clear. It can be seen from **Figure 3A** that for N-ZGyNR, the magnetic moments are mainly distributed on the atomic chains at the edges, the magnetic moments on the edge atomic chain presents an up-down staggered distribution, and the magnetic moments between the two edge chains are inverted symmetry. Therefore, as shown in **Figure 2A**, there will be spin degeneracy in N-ZGyNR.

When the Fe is doped into N-ZGyNR, it can be found from **Figure 3B** that, the spin distribution on the entire N-ZGyNR will be greatly affected. It can be seen that the magnetic moments on the middle C atom and N atom of the Fe-N-ZGyNR are significantly increased compared with the N-ZGyNR. The doped Fe atom breaks the original magnetic moment balance and changes the left-right symmetrical spin distribution of N-ZGyNR into an antisymmetrical distribution, and at the same time enhances the spin polarization. For example, the spin magnetic moment of C_1-C_7 in N-ZGyNR will increase from $\sim 0 \mu_B$ to 0.043, -0.063 , 0.021, -0.035 , -0.065 , 0.038, $-0.095 \mu_B$, respectively. In addition, there is a residual spin magnetic moment of about $1.69 \mu_B$ on the doped Fe atoms.

When the Co atom is doped into N-ZGyNR, similar to the case in the Fe-N-ZGyNR structure, the original magnetic moment

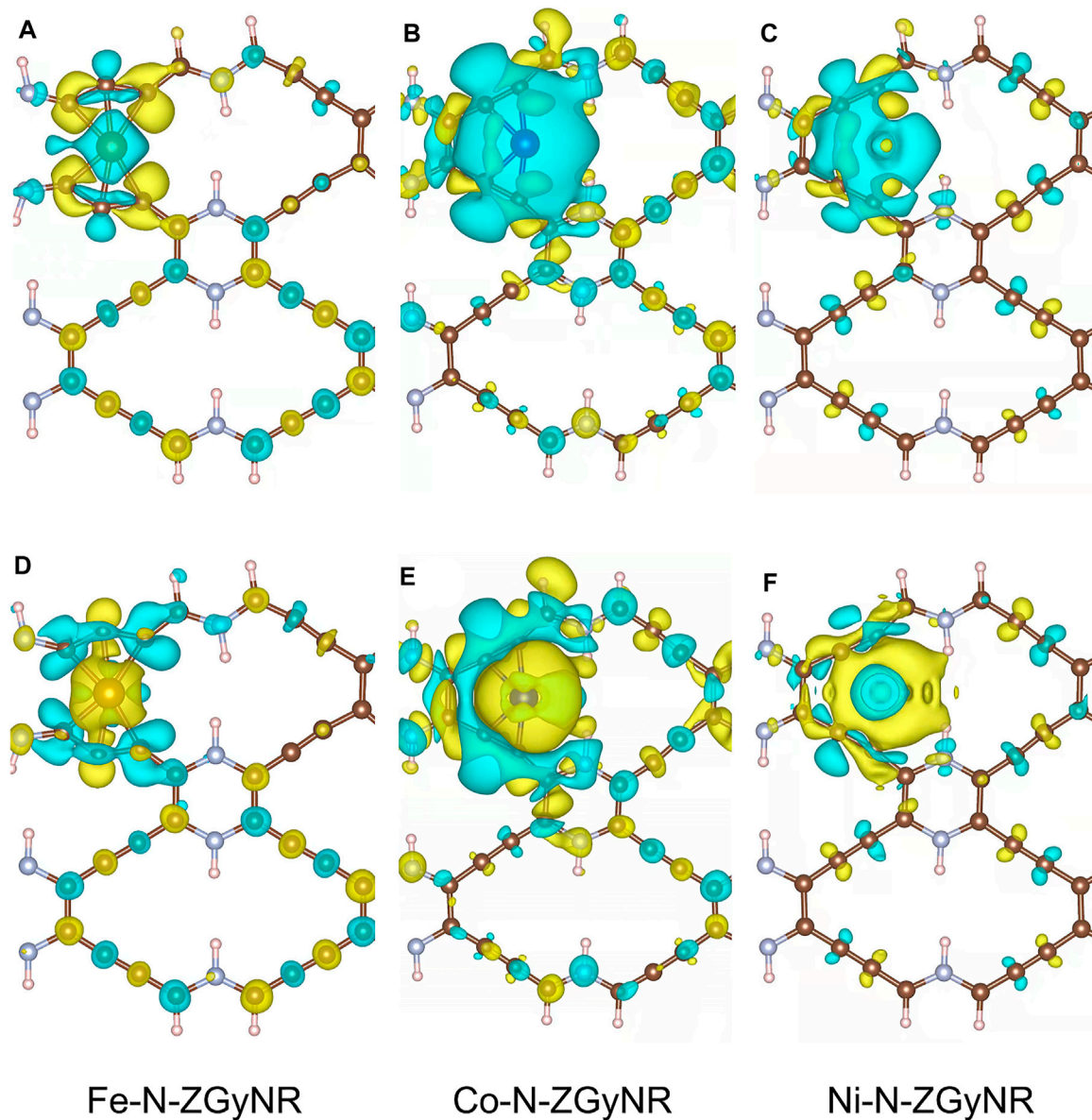


FIGURE 4 | The spin-up (A–C)/spin-down (D–F) electron density difference of M-N-ZGyNR (M = Fe, Co, Ni). The increase (decrease) of the spin electron magnetic moment is represented by the yellow (light blue) region. To make the comparison clear, the isosurface levels of Fe-N-ZGyNR, Co-N-ZGyNR and Ni-N-ZGyNR are set to $2 \times 10^{-3} e/\text{\AA}^3$, $2 \times 10^{-4} e/\text{\AA}^3$ and $8 \times 10^{-4} e/\text{\AA}^3$ respectively.

balance is broken and the magnetic moment of the original N-ZGyNR structure is affected. Different from Fe-N-ZGyNR, the influence of Co on the spin distribution of the N-ZGyNR is mainly limited to the C atoms adjacent to Co, such as C₂, C₃, C₆, C₇ (in **Figure 3C**). The spin-up electrons are mainly concentrated in the Co atoms, while the spin-down electrons are mainly concentrated in the C₂, C₃, C₆, C₇ atoms. The spin magnetic moments of C₂, C₃, C₆, C₇ and Co are -0.027 , -0.035 , -0.014 , -0.021 , $1.16 \mu_B$, respectively, which are smaller than the spin magnetic moment of Fe-N-ZGyNR but higher than that of N-ZGyNR. In addition, the spin magnetic moments on N₄ and C₃₂ will change from the reverse to the same direction,

which will hinder the spin charge transfer near the Fermi level, resulting in a band gap at the Fermi level, as shown in **Figure 2C**.

It is obvious from **Figure 3D** that when the Ni atom is doped into N-ZGyNR structure, the interaction between Ni and N-ZGyNR is weak (in **Figure 3D**). Compared with N-ZGyNR, the spin distribution in Ni-N-ZGyNR has changed but the intensity has not changed significantly (The isosurface level of **Figure 3D** is only an order of magnitude higher than **Figure 3A**), which is different from Fe and Co doping. Similar to Co-N-ZGyNR, the spin magnetic moments on C₁₅ and C₁₆, C₁₇ and C₁₈, C₃₁ and C₃₂ change from the reverse to the same direction. The overall result is that the electrical properties of Ni-N-ZGyNR are

basically the same as those of N-ZGyNR, maintaining the basic characteristics of the energy band, but opening the band gap near the Fermi level, as shown in **Figure 2D**.

Spin Electron Density Difference Analysis

Through the distribution of spin charge, we can find that the Fe doping has the greatest influence on the N-ZGyNR spin distribution, followed by Co doping and the Ni doping has the weakest influence. In order to study the spin charge transfer caused by the doping of magnetic atoms, the spin electron density difference $\Delta\rho^{\text{SEDD}}$ calculated by **Eq. 3** is shown in **Figure 4**. As a reference, the spin magnetic moments on isolated Fe, Co, and Ni atoms are 4, 3, 2 μ_B , respectively.

It can be found from **Figures 4A,D** that, when Fe atoms with 4 μ_B magnetic moment are doped into N-ZGyNR, the number of spin-up electrons on Fe atoms will decrease, and the number of spin-down electrons will increase. In addition, through bader charge analysis (**Supplementary Figure S3B**), it is found that about 0.8e⁻ will be transferred from Fe atoms to the N-ZGyNR structure. This will reduce the residual magnetic moment on the Fe atom to 1.69 μ_B , as shown in **Figure 3B**. The 0.8e⁻ transferred to N-ZGyNR are mainly captured by C₄ and C₅, which breaks the C₄(sp²) = C₅(sp²) bond. The secondary effect of charge transfer will change the spin distribution in the N-ZGyNR structure. For example, the spin-up charge on the C₁₆ atom located on the lower edge increases, and the spin-down charge decreases, which will strengthen the residual magnetic moment of the C₁₆ atom from 0.003 to 0.07 μ_B . The spin-up charge on the C₃₂ atom that is also located on the lower edge decreases, and the spin-down charge increases, which makes the residual magnetic moment of the C₃₂ atom reversely strengthened from 0.003 μ_B to -0.086 μ_B . Similar to Fe doping, when Co with a 3 μ_B magnetic moment is doped into N-ZGyNR, the spin-up charge of the Co atom itself will decrease, and the spin-down charge will increase (in **Figures 4B,E**). But only 0.6e⁻ are transferred from the Co atom to the N-ZGyNR (in **Supplementary Figure S3C**), which causes the magnetic moment of the Co atom to weaken from 3 to 1.16 μ_B . The 0.6e⁻ transferred to N-ZGyNR have significantly less influence on the original structure than Fe doping. For example, breaking C₂(sp)≡C₃(sp) into a C(sp)-C(sp) bond, increases the magnetic moment of N₈ at the lower edge from ~0 to 0.008 μ_B , which is the same as the direction of the magnetic moment of C₃₂. The effect of Ni doping on N-ZGyNR is minimal. The spin charge reversal of Ni atoms is limited to Ni atoms themselves, thereby eliminating the magnetic moment of Ni atoms (in **Figures 4C,F**), and there will be no charge transfer from Ni atoms to N-ZGyNR (in **Supplementary Figure S3D**). But the weak interaction between Ni and N-ZGyNR will also redistribute the spin on N-ZGyNR, such as flipping the magnetic moment on C₁₆ from 0.003 μ_B to -0.001 μ_B , which is the same as the direction of the magnetic moment on C₇.

CONCLUSION

In this work, the first-principles theory is used to study the effect of magnetic atom doping on the electrical properties of nitrogen-containing graphyne nanoribbon (N-ZGyNR). The results show

that different magnetic doping atoms have different effects on the structure and electrical properties of N-ZGyNR. When Fe atoms are doped, one of the C-C bonds will be completely broken, and the entire structure will undergo great structural distortion. With the transfer of about 0.8e⁻ from Fe atoms to the N-ZGyNR, the electrical properties of Fe-N-ZGyNR will change significantly. When Co atoms are doped, the influence on the N-ZGyNR is smaller than that of Fe doping. With the transfer of 0.6e⁻ electrons from the Co atom to the N-ZGyNR, the spin up-down alternating magnetic moment distribution at the N-ZGyNR edge will be broken, and a band gap of ~60 meV near the Fermi level in Co-N-ZGyNR will appear, thereby realizing the metal-semiconductor transition. The effect of Ni doping on the N-ZGyNR is the smallest among these three types of magnetic atom doping. There is no charge transfer from Ni to the N-ZGyNR, but the Van der Waals interaction between Ni and N-ZGyNR will also cause the magnetic moment redistribution in N-ZGyNR. Similar to the Co doping, an electronic band gap of about 60 meV is also generated near the Fermi level, which can also achieve a metal-semiconductor transition. The above results show that the electrical properties of N-ZGyNR can be controlled by magnetic atom doping, and the metal-semiconductor transition can be realized by Co/Ni doping, which provides a new alternative for spintronic devices.

DATA AVAILABILITY STATEMENT

The original contributions presented in the study are included in the article/**Supplementary Material**, further inquiries can be directed to the corresponding authors.

AUTHOR CONTRIBUTIONS

X-FP and S-HT organized the project, Z-CM completed the calculation and analysis of the results, and wrote the manuscript. All authors contributed to manuscript revision, read, and approved the submitted version.

FUNDING

This work was supported by the National Natural Science Foundation of China (Grant No. 11704417), by Hunan Provincial Natural Science Foundation of China (Grant No. 2019JJ40532), by Hunan Provincial Education Department research project, China (No. 17C1640), by the key projects of Hunan Provincial Department of Education (Grant No. 21A0167).

SUPPLEMENTARY MATERIAL

The Supplementary Material for this article can be found online at: <https://www.frontiersin.org/articles/10.3389/fmats.2022.854656/full#supplementary-material>

REFERENCES

- Baughman, R. H., Eckhardt, H., and Kertesz, M. (1987). Structure-property Predictions for New Planar Forms of Carbon: Layered Phases Containing Sp² and Sp Atoms. *J. Chem. Phys.* 87 (11), 6687–6699. doi:10.1063/1.453405
- Bhattacharya, B., Singh, N. B., and Sarkar, U. (2015). Tuning the Magnetic Property of Vacancy-Defected Graphyne by Transition Metal Absorption. *Struct. Chem.* 25, 1695. doi:10.1063/1.4917707
- Chang, C., Chen, W., Chen, Y., Chen, Y. H., Chen, Y., Ding, F., et al. (2021). Recent Progress on Two-Dimensional Materials. *Acta Phys. -Chim. Sin* 37 (12), 1–151. doi:10.3866/PKU.WHXB202108017
- Cocchi, C., Prezzi, D., Calzolari, A., and Molinari, E. (2010). Spin-transport Selectivity upon Co Adsorption on Antiferromagnetic Graphene Nanoribbons. *J. Chem. Phys.* 133, 124703–124705. doi:10.1063/1.3478317
- Deng, X. Q., Zhang, Z. H., Tang, G. P., Fan, Z. Q., and Yang, C. H. (2014). Spin Filter Effects in Zigzag-Edge Graphene Nanoribbons with Symmetric and Asymmetric Edge Hydrogenations. *Carbon* 66, 646–653. doi:10.1016/j.carbon.2013.09.061
- Donati, F., Gragnaniello, L., Cavallin, A., Natterer, F. D., Dubout, Q., Pivetta, M., et al. (2014). Tailoring the Magnetism of Co Atoms on Graphene through Substrate Hybridization. *Phys. Rev. Lett.* 113, 177201–177206. doi:10.1103/PhysRevLett.113.177201
- Dutta, S., Manna, A. K., and Pati, S. K. (2009). Intrinsic Half-Metallicity in Modified Graphene Nanoribbons. *Phys. Rev. Lett.* 102, 096601–096604. doi:10.1103/PhysRevLett.102.096601
- Haji-Nasiri, S., and Fotoohi, S. (2018). Doping Induced Diode Behavior with Large Rectifying Ratio in Graphyne Nanoribbons Device. *Phys. Lett. A* 382, 2894–2899. doi:10.1016/j.physleta.2018.08.007
- Jing, M., Wu, T., Zhou, Y., Li, X., and Liu, Y. (2020). Nitrogen-Doped Graphene via In-Situ Alternating Voltage Electrochemical Exfoliation for Supercapacitor Application. *Front. Chem.* 8, 428. doi:10.3389/fchem.2020.00428
- Kan, E.-j., Li, Z., Yang, J., and Hou, J. G. (2008). Half-Metallicity in Edge-Modified Zigzag Graphene Nanoribbons. *J. Am. Chem. Soc.* 130, 4224–4225. doi:10.1021/ja710407t
- Krause, R., Chávez-Cervantes, M., Aeschlimann, S., Forti, S., Fabbri, F., Rossi, A., et al. (2021). Ultrafast Charge Separation in Bilayer WS₂/Graphene Heterostructure Revealed by Time- and Angle-Resolved Photoemission Spectroscopy. *Front. Phys.* 9, 668149. doi:10.3389/fphys.2021.668149
- Kresse, G., and Furthmüller, J. (1996). Efficient Iterative Schemes For Ab Initio Total-Energy Calculations Using a Plane-Wave Basis Set. *Phys. Rev. B* 54, 11169–11186. doi:10.1103/PhysRevB.54.11169
- Kresse, G., and Joubert, D. (1999). From Ultrasoft Pseudopotentials to the Projector Augmented-Wave Method. *Phys. Rev. B* 59, 1758–1775. doi:10.1103/PhysRevB.59.1758
- Lazić, P., and Crljen, Ž. (2015). Graphyne on Metallic Surfaces: A Density Functional Theory Study. *Phys. Rev. B* 91, 125423–125425. doi:10.1103/PhysRevB.91.125423
- Li, X., and Zhang, G. (2013). Enhancing the Extremely High thermal Conduction of Graphene Nanoribbons. *Front. Phys.* 1, 19. doi:10.3389/fphys.2013.00019
- Li, Y., Xu, L., Liu, H., and Li, Y. (2014). Graphdiyne and Graphyne: from Theoretical Predictions to Practical Construction. *Chem. Soc. Rev.* 43, 2572. doi:10.1039/c3cs60388a
- Li, J., Zhang, Z. H., Wang, D., Zhu, Z., Fan, Z. Q., Tang, G. P., et al. (2014). Electronic Structures, Field Effect Transistor and Bipolar Field-Effect Spin Filtering Behaviors of Functionalized Hexagonal Graphene Nanoflakes. *Carbon* 69, 142–150. doi:10.1016/j.carbon.2013.11.076
- Li, Z., Xie, W., Liu, X., and Wu, Y. (2015). Magnetic Property and Possible Half-Metal Behavior in Co-doped Graphene. *J. Appl. Phys.* 117, 084311–084315. doi:10.1063/1.4913387
- Li, H., Chen, T., Zhu, Y., Yan, S., and Zhou, G. (2020). Spin Multiple Functional Devices in Zigzag-Edged Graphyne Nanoribbons Based Molecular Nanojunctions. *J. Magnetism Magn. Mater.* 498, 166223. doi:10.1016/j.jmmm.2019.166223
- Lin, X., and Ni, J. (2011). Half-metallicity in Graphene Nanoribbons with Topological Line Defects. *Phys. Rev. B* 84, 075461–075464. doi:10.1103/PhysRevB.84.075461
- Lin, Z.-Z., Wei, Q., and Zhu, X. (2014). Modulating the Electronic Properties of Graphdiyne Nanoribbons. *Carbon* 66, 504–510. doi:10.1016/j.carbon.2013.09.027
- Liu, W., Cao, T., Dai, X., Bai, Y., Lu, X., Li, F., et al. (2021). Nitrogen-Doped Graphene Monolith Catalysts for Oxidative Dehydrogenation of Propane. *Front. Chem.* 9, 835. doi:10.3389/fchem.2021.759936
- Malko, D., Neiss, C., Viñes, F., and Görling, A. (2012). Competition for Graphene: Graphynes with Direction-dependent Dirac Cones. *Phys. Rev. Lett.* 108, 086804. doi:10.1103/PhysRevLett.108.086804
- Momma, K., and Izumi, F. (2011). VESTA 3 for Three-Dimensional Visualization of crystal, Volumetric and Morphology Data. *J. Appl. Cryst.* 44, 1272–1276. doi:10.1107/S0021889811038970
- Narita, N., Nagai, S., Suzuki, S., and Nakao, K. (1998). Optimized Geometries and Electronic Structures of Graphyne and its Family. *Phys. Rev. B* 58, 11009–11014. doi:10.1103/physrevb.58.11009
- Nayebi, P., and Shamshirsaz, M. (2020). Effect of Vacancy Defects on Transport Properties of α -armchair Graphyne Nanoribbons. *Eur. Phys. J. B* 93, 170. doi:10.1140/epjb/e2020-10183-5
- Pan, J., Du, S., Zhang, Y., Pan, L., Zhang, Y., Gao, H.-J., et al. (2015). Ferromagnetism and Perfect Spin Filtering in Transition-Metal-Doped Graphyne Nanoribbons. *Phys. Rev. B* 92, 205429. doi:10.1103/PhysRevB.92.205429
- Puigdollers, A. R., Alonso, G., and Gamallo, P. (2016). First-principles Study of Structural, Elastic and Electronic Properties of α -, β - and γ -graphyne. *Carbon* 96, 879–887. doi:10.1016/j.carbon.2015.10.043
- Qi, S., Ma, X., Yang, B., Sun, L., Li, W., and Zhao, M. (2019). Two-dimensional Graphyne-like Carbon Nitrides: Moderate Band Gaps, High Carrier Mobility, High Flexibility and Type-II Band Alignment. *Carbon* 149, 234–241. doi:10.1016/j.carbon.2019.04.024
- Ren, K., Ren, C., Luo, Y., Xu, Y., Yu, J., Tang, W., et al. (2019). Using van der Waals heterostructures based on two-dimensional blue phosphorus and XC (X = Ge, Si) for water-splitting photocatalysis: a first-principles study. *Phys. Chem. Chem. Phys.* 21, 9949–9956. doi:10.1039/C8CP07680D
- Sarma, J. V. N., Chowdhury, R., and Jayaganthan, R. (2014). Graphyne-based Single Electron Transistor: Ab Initio Analysis. *Nano* 09, 1450032. doi:10.1142/S1793292014500325
- Sevinçli, H., and Sevik, C. (2014). Electronic, Phononic, and Thermoelectric Properties of Graphyne Sheets. *Appl. Phys. Lett.* 105, 223108. doi:10.1063/1.4902920
- Son, Y.-W., Cohen, M. L., and Louie, S. G. (2006). Half-metallic Graphene Nanoribbons. *Nature* 444, 347–349. doi:10.1038/nature05180
- Wang, C., Ouyang, T., Chen, Y., and Zhong, J. (2015). Enhancement of Thermoelectric Properties of Gamma-Graphyne Nanoribbons with Edge Modulation. *Eur. Phys. J. B* 88, 130. doi:10.1140/epjb/e2015-60153-y
- Wang, D., Zhang, Z. H., Deng, X. Q., Fan, Z. Q., and Tang, G. P. (2016). Magnetism and Magnetic Transport Properties of the Polycrystalline Graphene Nanoribbon Heterojunctions. *Carbon* 98, 204–212. doi:10.1016/j.carbon.2015.10.090
- Wang, Y., Huang, Y., Song, Y., Zhang, X., Ma, Y., Liang, J., et al. (2009). Room-Temperature Ferromagnetism of Graphene. *Nano Lett.* 9 (1), 220–224. doi:10.1021/nl802810g

- Wu, W., Guo, W., and Zeng, X. C. (2013). Intrinsic Electronic and Transport Properties of Graphyne Sheets and Nanoribbons. *Nanoscale* 5, 9264. doi:10.1039/c3nr03167e
- Xi, J., Wang, D., Yi, Y., and Shuai, Z. (2014). Electron-phonon Couplings and Carrier Mobility in Graphynes Sheet Calculated Using the Wannier-Interpolation Approach. *J. Chem. Phys.* 141, 034704–034711. doi:10.1063/1.4887538
- Young, S. M., and Kane, C. L. (2015). Dirac Semimetals in Two Dimensions. *Phys. Rev. Lett.* 115, 126803. doi:10.1103/PhysRevLett.115.126803
- Yue, Q., Chang, S., Kang, J., Tan, J., Qin, S., and Li, J. (2012). Magnetic and Electronic Properties of α -graphyne Nanoribbons. *J. Chem. Phys.* 136, 244702. doi:10.1063/1.4730325
- Zakharov, A. A. (2021). Ambipolar Behavior of Ge-Intercalated Graphene: Interfacial Dynamics and Possible Applications. *Front. Phys.* 9, 101. doi:10.3389/fphy.2021.641168
- Zhang, S., and Ma, J. (2011). Width- and Edge-dependent Stability, Electronic Structures, and Magnetic Properties of Graphene-like and Wurtzite ZnS Nanoribbons. *J. Phys. Chem. C* 115, 4466–4475. doi:10.1016/j.physe.2014.01.00310.1021/jp110148m
- Zhao, C.-C., Tan, S.-H., Zhou, Y.-H., Wang, R.-J., Wang, X.-J., and Chen, K.-Q. (2017). Half-metallicity and High Spin-Filtering Effect of Magnetic Atoms Embedded Zigzag 6, 6, 12-graphyne Nanoribbon. *Carbon* 113, 170–175. doi:10.1016/j.carbon.2016.11.022

Conflict of Interest: The authors declare that the research was conducted in the absence of any commercial or financial relationships that could be construed as a potential conflict of interest.

Publisher's Note: All claims expressed in this article are solely those of the authors and do not necessarily represent those of their affiliated organizations, or those of the publisher, the editors and the reviewers. Any product that may be evaluated in this article, or claim that may be made by its manufacturer, is not guaranteed or endorsed by the publisher.

Copyright © 2022 Min, Peng and Tan. This is an open-access article distributed under the terms of the Creative Commons Attribution License (CC BY). The use, distribution or reproduction in other forums is permitted, provided the original author(s) and the copyright owner(s) are credited and that the original publication in this journal is cited, in accordance with accepted academic practice. No use, distribution or reproduction is permitted which does not comply with these terms.